# A Numerical Study of Combined Natural and Marangoni Convection in a Square Cavity

## K. Cicek & A. Cihat Baytas
**Istanbul Technical University, Tuzla, Istanbul, Turkey**

ABSTRACT: Through the aim of this study, the effects of combined buoyancy-driven flows and thermo capillary flows, which are emerged from temperature differences, on fluid flow and heat transfer numerically investigated with differentially heated side walls in a free surface square cavity. The study has been accomplished with three milestones to achieve the right solutions. For every milestone Navier-Stokes, continuity and energy equations are discretized by using finite volume method and grids with 52 x 52 control volumes. Results are presented Pr=1, Pr=7 and Pr=100. The effect of positive and negative Marangoni number on fluid flow and heat transfer at different Rayleigh number are considered and discussed.

NOMENCLATURE

$c_p$ : specific heat at a constant pressure J/(kg-K)
D : height of cavity, m
g : gravitational acceleration, $m^2$/s
h : convection heat transfer coefficient, W/($m^2$-K)
k : thermal conductivity, W/(m-K)
p : pressure, N/$m^2$
$q''$ : heat flux, W/$m^2$
t : time, s
T : temperature, K
u : horizontal velocity, m/s
U : dimensionless horizontal velocity
v : vertical velocity, m/s
V : dimensionless vertical velocity
x,y : coordinates, m
X : dimensionless horizontal coordinate
Y : dimensionless vertical coordinate
$\Delta T$ : temperature difference ($T_H$-$T_C$)
$\alpha$ : thermal diffusivity, $m^2$/s
$\beta$ : thermal expansion coefficient, 1/K
$\theta$ : dimensionless temperature
$\mu$ : dynamic viscosity, kg/(m-s)
$\nu$ : kinematics viscosity, $m^2$/s
$\rho$ : density, kg/$m^3$
$\sigma$ : surface tension, N/m
$\sigma T$ : temperature coefficient of surface tension, N/(m-K)
$\tau$ : dimensionless time
$\psi$ : stream function, $m^2$/s
$\Psi$ : dimensionless stream function
$\omega$ : vorticity, 1/s
$\Omega$ : dimensionless vorticity

*Dimensionless Numbers*
Pr: Prandtl number
Ra : Rayleigh number
Ma : Marangoni number
$\underline{Nu}$ : Nusselt number
$\overline{Nu}$ : Average Nusselt number
Pe : Peclet number

*Subscripts*
H : hot
C : cold
l : local

## 1 INTRODUCTION

From its modest origins, maritime transportation has always been the dominant support of global trade. Therewithal, the importance of maritime transportation increases in parallel with technologic evolutions, technical improvements and economic development of countries. High level of economic growth, industrialization, technological evolutions and urbanization for developed countries result in an increase in energy demand. It was determined that in 2005, 86% of primary energy demand in the world supplied from petroleum and derivatives. Therefore, maritime transportation is the most important transportation mode for transferring of petroleum and its derivatives to procure energy demand. With the current data illustrated that transportation of fossil fuels by seaway reached approximately twenty seven billion tons in the year 2007 (UNCTAD, 2007).

Increase in the volume of carriage of petroleum and its derivatives with maritime transportation have increased the risk of the maritime accidents such as oil spill, collision, grounding of ships that threaten to environment, ecosystems, and aquatic life. For this reason many academic researches and studies are directly focused out on prevention of pollution of marine environment with exploring fluid mechanics and heat transfer events in cargo tanks of ships such as Grau et al. 2004, Oro et al. 2006, Pallares et al. 2004, Segerre-Perez et al. 2007.

The main aim of present study is to shed light on fluid flow and heat transfer in cargo tank of ships. The present work is a numerical study natural convection due to the temperature difference between left and right wall and Marangoni convection due to the free surface effect in a two-dimensional square cavity. Natural convection is induced by the difference in temperature between vertical walls, and it is represented by the Rayleigh number (Ra). Marangoni convection flow directly related to the surface tension gradient with respect to temperature which acts as a force applied to the free surface of the cavity, and it is represented by the Marangoni number (Ma). The presence of free surface can not only alter the flow field and heat transfer but also prove to have an impact on the process because of surface tension variations (Behnia, Stella, Guj 1995; Bergman & Ramadhyani 1986; Smith & Davis 1983).

The study is conducted numerically under the assumption of steady laminar flow with three milestones. In the first milestone, natural convection in a two-dimensional square cavity has been investigated with the left vertical wall is a constant temperature $T_h$, the right wall is constant $T_c$ and all other walls are assumed adiabatic. In the second milestone, combined natural and Marangoni convection in a two-dimensional square cavity with a top free surface has been investigated with the left vertical wall is a constant temperature $T_h$, the right wall is constant $T_c$, and all other walls are adiabatic. In the third and last milestone combined natural and Marangoni convection in a two-dimensional square cavity with a top free surface has been investigated with the left vertical wall is a constant temperature $T_c$, the right and bottom wall is constant $T_c$, whilst top surface is adiabatic. For the second and third milestones, the top surface deformation and interactions with the gaseous phase are neglected. In every three steps, the Navier-Stokes, continuity and energy equations are solved using finite volume method and grids with 52 x 52 control volumes. Results are presented Pr=7 for first and second milestones, Pr=100 for third milestone. The effect of positive and negative Marangoni number on the fluid flow and heat transfer at different Rayleigh numbers are considered and discussed.

## 2 MATHEMATICAL MODEL

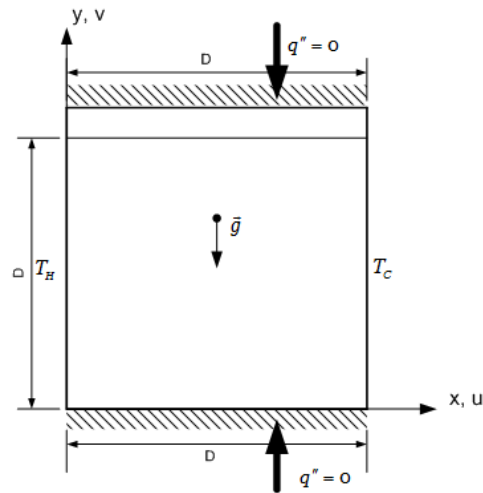A schematic diagram of every milestone shows in Figure 1, Figure 2 and Figure 3 respectively.



Figure 1. Schematic diagram of the physical model and coordinate system of first milestone.
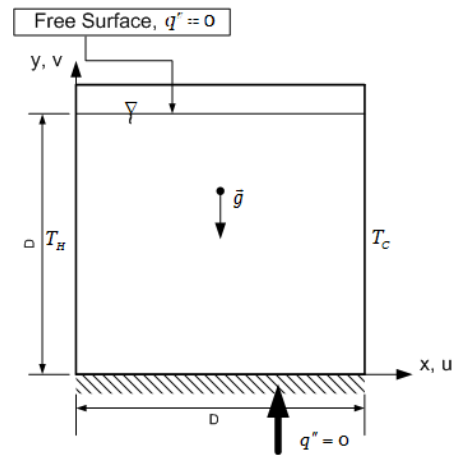


Figure 2. Schematic diagram of the physical model and coordinate system of second milestone.
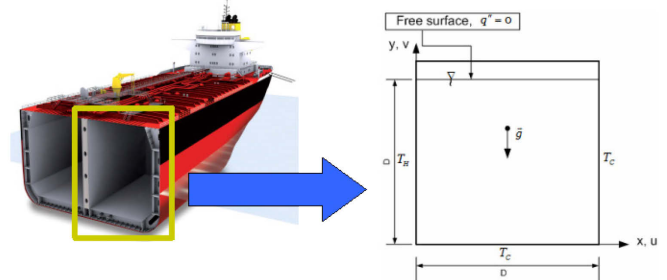


Figure 3. Schematic diagram of the physical model and coordinate system of third milestone.

In Figure 1, it is assumed that the left vertical wall of the cavity is a constant value $T_H$. The right vertical wall is held at a constant temperature $T_C$, while the horizontal walls are adiabatic. In Figure 2, it is assumed that the left vertical wall of the cavity is a constant value $T_H$. The right vertical wall is held at a constant temperature $T_C$, top horizontal wall is a

free surface and adiabatic and bottom horizontal wall is adiabatic. In Figure 3, cargo tank is modeled to investigate fluid motion and heat transfer in tank. In Figure 3, it is assumed that the left vertical wall of the cavity is a constant value $T_H$. The right vertical wall and bottom horizontal walls are held at a constant temperature $T_C$, while the top horizontal wall is a free surface and adiabatic.

To model the liquid motion in cavity, we use the conservation equation for mass, momentum and energy for two-dimensional, steady and laminar flow. All the physical properties of fluid, $\mu$, $k$ and $c_p$ are considered constant except density, in buoyancy term, which obeys Boussinesq approximation. In the energy conservation, we neglect the effect of compressibility and viscous dissipation. With these assumptions the continuity, momentum and energy equations can be written as;

$$\frac{\partial u}{\partial x} + \frac{\partial v}{\partial y} = 0 \tag{1}$$

$$\rho \frac{dv}{dt} = \rho g - \nabla P + \mu \nabla^2 v \tag{2}$$

$$\frac{\partial T}{\partial t} + u \frac{\partial T}{\partial x} + v \frac{\partial T}{\partial y} = \alpha \left[ \frac{\partial^2 T}{\partial x^2} + \frac{\partial^2 T}{\partial y^2} \right] \tag{3}$$

Introducing the vorticity w as;

$$w = \nabla \times v \tag{4}$$

to get vorticity transport equation by taking the curl of momentum equation to eliminates the $\nabla P$ term, the momentum equation can be rewritten in terms of the vorticity defined above as;

$$\frac{\partial \omega}{\partial t} + u \frac{\partial \omega}{\partial x} + v \frac{\partial \omega}{\partial y} = \nu \nabla^2 \omega + g \beta \frac{\partial T}{\partial x} \tag{5}$$

The stream function ($\psi$) for two dimensional problem is defined such that;

$$v = \nabla \times \psi \tag{6}$$

the vorticity transport equation can be obtained from Eqs. (5) and (6), which further gives;

$$\omega = -\nabla^2 \psi \tag{7}$$

The governing equations are converted into the non-dimensional form by defining the non-dimensional variables:

$$X = \frac{x}{D},\ Y = \frac{y}{D},\ U = \frac{uD}{\alpha},\ \text{V} = \frac{vD}{\alpha},\ \Omega = \frac{\omega D^2}{\alpha}$$
$$\Psi = \frac{\psi}{\alpha},\ \theta = \frac{T - T_s}{\Delta T},\ \tau = \frac{t\alpha}{D^2},\ Ra = \frac{g\beta\Delta T D^3}{\nu\alpha},\ \text{Pr} = \frac{\nu}{\alpha} \tag{8}$$

Based on these non-dimensional variables, the governing equations are obtained as follow;

$$\frac{\partial U}{\partial X} + \frac{\partial V}{\partial Y} = 0 \tag{9}$$

$$\frac{\partial \Omega}{\partial \tau} + U \cdot \frac{\partial \Omega}{\partial X} + V \cdot \frac{\partial \Omega}{\partial Y} = \text{Pr} \cdot \left[ \frac{\partial^2 \Omega}{\partial X^2} + \frac{\partial^2 \Omega}{\partial Y^2} \right] + Ra \cdot \text{Pr} \cdot \frac{\partial \theta}{\partial X} \tag{10}$$

$$\frac{\partial \theta}{\partial \tau} + U \cdot \frac{\partial \theta}{\partial X} + V \cdot \frac{\partial \theta}{\partial Y} = \nabla^2 \theta \tag{11}$$

$$-\Omega = \nabla^2 \Psi \tag{12}$$

$$U = \frac{\partial \Psi}{\partial Y},\ \text{V} = -\frac{\partial \Psi}{\partial X} \tag{13}$$

Other physical quantities of interest in the present study are the average and local Nusselt numbers for the hot and cold walls; these variables are defined respectively as;

$$Nu_{l(hot)} = -\frac{\partial \theta}{\partial X}\bigg|_{x=0},\ Nu_{l(cold)} = -\frac{\partial \theta}{\partial X}\bigg|_{x=D} \tag{14}$$

$$\overline{Nu} = -\int_0^1 \frac{\partial \theta}{\partial X} dY = -\int_0^1 Nu_l dY \tag{15}$$

# 3  INITIAL & BOUNDARY CONDITIONS

In order to obtain results of the conservation equations we define initial and boundary conditions. For each milestone initial conditions are at $\tau = 0$;

$$U = V = \theta = \Psi = \Omega = 0$$

But it is necessary to define boundary conditions of each milestone separately. In first milestone the boundary conditions are at $\tau \geq 0$;

$X = 0$, $0 \leq Y \leq 1$, $U = V = \Psi = 0$ & $\theta = 1$ (16a)

$X = 1$ ve $0 \leq Y \leq 1$ de $U = V = \Psi = 0$ & $\theta = 0$ (16b)

$Y = 0$, $0 \leq X \leq 1$, $U = V = \Psi = 0$ & $\dfrac{\partial \theta}{\partial Y} = 0$ (16c)

$Y = 1$ ve $0 \leq X \leq 1$ de $U = V = \Psi = 0$ & $\dfrac{\partial \theta}{\partial Y} = 0$ (16d)

Also it is necessary to define non-dimensional vorticity boundary conditions and with the help of Eqs. (4) the boundary conditions can be obtained as for vertical walls;

$$\Omega = -\frac{\partial^2 \Psi}{\partial X^2} \tag{16e}$$

and for horizontal walls;

$$\Omega = -\frac{\partial^2 \Psi}{\partial Y^2} \tag{16f}$$

In the second and third milestones free surface condition must be taken in consideration. The presence of this type of boundary condition can not only alter the flow field and heat transfer characteristics but may also prove to have an impact on the process because of surface tension variations. (Smith & Davis 1983; Bergman & Ramadhyani 1986). In general, for most liquids there is a variation of surface tension with temperature. As a result, the interface between air and liquid which is subjected to a temperature gradient can initiate a bulk flow due to surface tension variations. This flow which is due to a temperature gradient applied normally to the free surface is known as Marangoni convection (Behnia et al 1995). After that explanation, the boundary condition at a free surface can be written as,

$$\left.\frac{\partial u}{\partial y}\right|_{y=D} = \frac{1}{\mu} \cdot \frac{\partial \sigma}{\partial T} \cdot \left.\frac{\partial T}{\partial x}\right|_{y=D} \quad (17)$$

Based on non-dimensional variables expressed in Eqs (8), Eqs 17 are obtained as follow;

$$\frac{\partial U}{\partial Y} = Ma\frac{\partial \theta}{\partial X} \quad (18)$$

$$Ma = -\frac{d\sigma}{dT}\frac{\Delta TD}{\mu\alpha}, \quad \frac{d\sigma}{dT} = \sigma_T$$

Eqs. (18) can be rearranged with the help of

$$U = \frac{\partial \Psi}{\partial Y}, \quad V = -\frac{\partial \Psi}{\partial X}$$

and obtained as follow;

$$\frac{\partial^2 \Psi}{\partial Y^2} = Ma\frac{\partial \theta}{\partial X} \quad (19)$$

This boundary condition applied to a vorticity boundary condition for top horizontal wall as follow;

$$\Omega = -\frac{\partial^2 \Psi}{\partial Y^2} = -Ma\frac{\partial \theta}{\partial X} \quad (20)$$

In the second milestone initial and boundary conditions are same with the first milestone except top horizontal wall (free surface condition).

In the third milestone initial and boundary conditions are same with the second milestone except bottom horizontal wall. In this milestone the bottom wall is held to a constant temperature $T_c$. For this reason the boundary condition for bottom wall is defined as follow,

$$Y = 0, 0 \leq X \leq 1, U = V = \Psi = 0 \ \& \ \theta = 0 \quad (21)$$

## 4 SOLUTION PROCEDURE

The differential equations, represented by equations (9) to (11), together with respect boundary conditions for every milestone, equations are (16), (20) and (21), are solved using the fine volume method described in Patankar (1980). In this method solution domain is divided into small finite control volumes. The differential equations are integrated into each of those control volumes. From this integration there were algebraic equations which, when solved simultaneously or separately, supplied velocity, stream function, vorticity and temperature components. A power-law scheme is adopted for the convection-diffusion formulation (Patankar 1980).

The discretization equations are solved iteratively, using the line by line method known as Thomas algorithm or TDMA (tridiagonal matrix algorithm). An over relaxation parameter of 1.85 was used in order to obtain stable convergence for the solution of vorticity transport and energy equations.

In order to assess the accuracy of our numerical procedure for every milestone, we have tested our algorithm based on the grid size (42 X 42) for the first milestone with the work of Davis (1983a), Davis (1983b) and Hortman and Peric (1990), for the second milestone we have tested our algorithm based on the grid sizes (52 X 52) with the work of Behnia et al (1995).

Grid independence tests were conducted for all the configurations studied in this work. Three different grid size (42 X 42, 52 X 52, 62 X 62) were used and average Nusselt numbers are compared for different grid size. Because of the small differences between 52 X 52 and 62 X 62 grids, 52 X 52 grid was chosen for second and third milestones. For the first milestone 42 X 42 grid was chosen because of achieve effective benchmark with the work of Davis (1983a), Davis (1983b) and Hortman and Peric (1990). The numerical solution is considered to be converged when the maximum convergence criteria was smaller than $10^{-7}$

## 5 NUMERICAL RESULTS AND DISCUSSION

In Figure 4 illustrate the stream function and isotherm contours of first milestone numerical results for various Ra=$10^3$ and $10^5$ and Pr=1. In general, fluid circulation is strongly dependent on Rayleigh number as we have seen in Figure 4a and 4b. Change in the values of Ra has its influence on the stream lines and isotherms. The centre of circulation pattern moved towards to hot (left) wall of the cavity. Streamlines pattern shows that there is a strong upward flow near the hot wall side and downward flow near the cold wall.

(a)

(b)

Figure 4. Stream lines and isotherm contours for (a) Ra=103, (b) Ra=105

In Figure 5-7 illustrate the stream function and isotherm contours of second milestone numerical results for Ra=0 and $10^4$, Ma=$\pm 10^3$ and Pr=7.



Figure 5. Stream lines and isotherm contours for Ra=0, Ma=$10^3$



Figure 6. Stream lines and isotherm contours for Ra=$10^4$, Ma=$10^3$



Figure 7. Stream lines and isotherm contours for Ra=$10^4$, Ma=-$10^3$

In general, fluid circulation is strongly dependent on both Rayleigh number and Marangoni number as we have seen in Figure 5-7. Change in the values of Ra and Ma have influence on the stream lines and isotherms. In Figure 5 only the effects of surface tension are present, the Rayleigh number being set to zero. The flow is driven due to effect of velocity gradients on the top surface. In Figure 6 it is seen that the effect of buoyancy on the flow field is added to the positive Marangoni one. So the flow structure is still constituted by a single large main circulation. Due to the effect of buoyancy forces that are distributed in the bulk of the cavity the main vortex is stronger than in Figure 5 and encompasses almost completely the entire flow domain. For positive Ma there is a strong thermal boundary layer located close to the upper-right corner due to the effect of Marangoni convection in the vicinity of the free surface. In Figure 7, due to the negative value of Marangoni number, there is an opposition of effects between buoyancy and surface tension. For this reason, it is possible to clearly distinguish the effect of the two different contributions. In this case, it is clearly evident how the flow is strongly divided into two regions; the upper one where the motion is induced by surface tension and the lower one driven by buoyancy. Also in Figure 7 isotherm contours shows that the negative Ma causes a strong penetration of hot fluid in the centre of the cavity due to the combined effect of the two counter-rotating recirculation.

In Figure 8-10 illustrate the stream function and isotherm contours of third and last milestone numerical results for Ra=0 and $10^4$, Ma=$\pm 10^3$ and Pr=100.
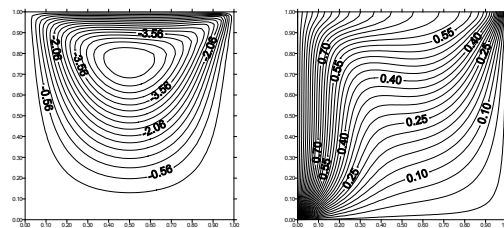


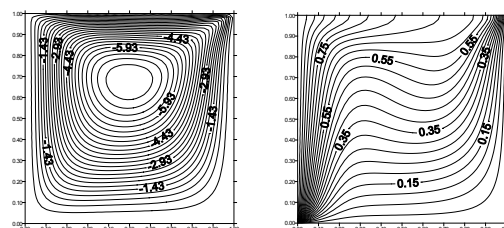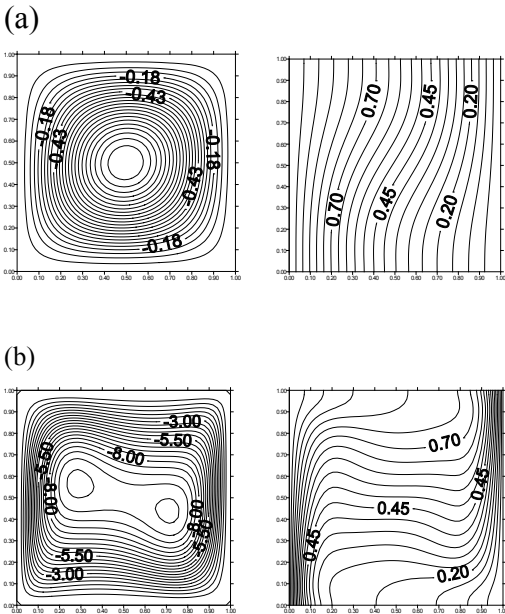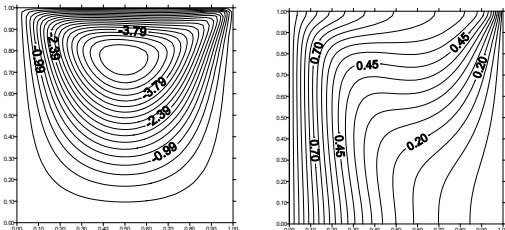Figure 8. Stream lines and isotherm contours for Ra=0, Ma=$10^3$
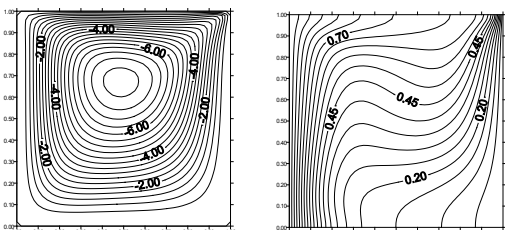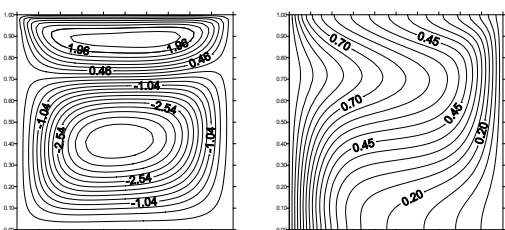


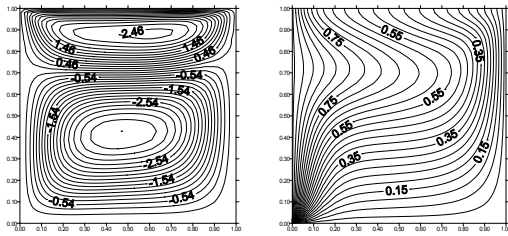Figure 9. Stream lines and isotherm contours for Ra=$10^4$, Ma=$10^3$

Figure 10. Stream lines and isotherm contours for Ra=10$^4$, Ma=-10$^3$

The bottom wall which is held at a constant temperature $T_C$ doesn't make any changes on stream line contours but have influence on the isotherm contours. As a result there is a strong boundary layer located close to lower-left corner. In Figure 8-10 stream lines contours don't show any difference but isotherm contours with the influence of bottom wall show significance varieties.

## 6 CONCLUSION

This study try to shed light on fluid flow and heat transfer in cargo tank of ships with investigating of combined natural and Marangoni convection in a liquid.

For the case of positive Marangoni number the fluid structure is mainly constituted by a dominant core vortex structure which becomes stronger as either of the Rayleigh and Marangoni numbers are increased.

More complex and interesting is the flow structure for negative values of Marangoni numbers. In this case, the fluid is stratified and flow filed is clearly divided into two separate regions where the motion is driven by Marangoni (upper region) and buoyancy (lower region) respectively.

Also for the bottom wall at a constant temperature $T_c$, it is shown that there is a strong thermal boundary layer is formed at the lower-left corner. It is clearly evident of lower-left corner is a strong heat loss point.

Consequently, Marangoni number is as important parameter as Rayleigh number for fluid motion and dispersion of temperature in cavity with free surface and for positive and negative values it changes both stream lines and isotherms contours dispersion in the cavity.

## REFERENCES

Behnia, M., Stella, F., & Guj, G. 1995. A numerical study of three dimensional combined buoyancy and thermocapillary convection, *International Journal of Multiphase Flow,* 21(3): 529-542.

Bergman, T.L. & Ramadhyani, S. 1986. Combined buoyancy and thermocapillary driven convection in open square cavities. *Journal of Numerical Heat Transfer,* 9: 441-451.

Bergman, T.L. and Keller, J.R., 1988. Combined Buoyancy, Surface Tension Flow in Liquid Metals, Numerical Heat Transfer, 13, 49-63.

Davis, G.D.V., 1983a, Natural Convection of Air in a Square Cavity: A Bench Mark Numerical Solution, International Journal for Numerical Methods in Fluids, 3, 249-264.

Davis, G.D.V., 1983b, Natural Convection of Air in a Square Cavity: A Comprasion Exercise, International Journal for Numerical Methods in Fluids, 3, 227-248.

Faghri, A. and Zhang, Y., 2006. Transport phenomena in multiphase systems. Academic Press, London.

Grau, F.X., Valencia, L., Fabregat, A., Pallares, J. and Cuesta I., 2005. Modelization and simulation of the fluid dynamics of the fuel in sunken tankers and of the dispersion of the fuel spill, *Symposium on Marine Accidental Oil Spills*, Vigo, Spain, July 13-16.

Hortman, M. and Peric, M., 1990. Finite volume multigrid prediction of laminar narutal convection: bench-mark solution, International Journal for Numerical Methods in Fluids, 11, 189-207.

Oro, J.M.F., Morros, C.S. and Diaz, K.M.A., 2006. Numerical simulation of the fuel oil cooling process in a wrecked ship, *Journal of Fluid Engineering,* 128, 1390-1393.

Pallares J., Cuesta I. and Grau F.X., 2004. Numerical simulation of the fuel oil cooling in the sunken prestige tanker. The ASME-ZSIS *International Thermal Science Seminar II,* Bled, Slovenia, June 13-16, 439-445.

Patankar, S.V., 1980. Numerical Heat Transfer and Fluid Flow, Hemissphere Publishing Corporation, Washington D.C.

Segerra-Perez, C.D., Olivia, A., Trias, X., Lehmkuhl, O. and Capdevila, A., 2007. Numerical simulation of thermal and fluid dynamic behavior of fuel oil in sunken ships, *Symposium on Marine Accidental Oil Spills,* Vigo, Spain, June 5-8, 31.

Smith, M.K. & Davis, S.H. 1983. Instabilities of dynamic thermocapillary liquid layers, part 1. Convective instabilities. *Journal of Fluid Mechanics,* 132: 119-144.